10 Lepton-Quark Scattering

Quantum electrodynamics is well understood for electrons and positrons. Thus electrons are ideal to probe the structure of mesons and baryons. Here we discuss the scattering of electrons off protons which historically was essential in establishing the substructure of hadrons.

10.1 Proton Structure

We start with elastic electron-proton scattering $e^- p \to e^- p$ where the proton recoils from the impacting electron. If the proton were a point-like particle with spin $\frac{1}{2}$ and charge $+e$ this process would described by the same formalism as in $e^-\mu^- \to e^-\mu^-$ scattering discussed earlier, see Mott- and Rutherford cross sections, Equations 176 and 177. Since the electron is point-like indeed, this process has been studied to probe the charge distribution inside the proton, as is shown in Figure 45. The blob describes the charge distribution of the proton. The difference to the cross

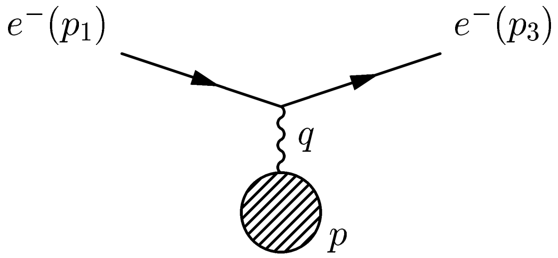

Figure 45: Charge distribution of a proton.

section of $e^- p \to e^- p$ scattering to the cross section from a point charge target is described by the **form factor** $F(q^2)$:

$$\frac{\mathrm{d}\sigma}{\mathrm{d}\Omega} = \left.\frac{\mathrm{d}\sigma}{\mathrm{d}\Omega}\right|_{\text{point}} \mid F(q^2) \mid^2$$

It follows that $F(q^2 = 0) = 1$. The form factor $F(q^2)$ is found to be decreasing as a function of the momentum transfer q^2. The larger q^2 the deeper inside the proton the scattering takes place. In essence, $\mid F(q^2) \mid^2$ measures the probability that the proton scatters as whole off the impacting electron. At large q^2 this is found to be very improbable.

Mathematically, the form factor is defined as the Fourier transform of charge distribution $\varrho(\vec{x})$ inside the proton

$$F(q^2) = \int \varrho(\vec{x}) \exp(i\vec{q}\cdot\vec{x}) \mathrm{d}^3x \tag{182}$$

For small values of q^2, we can expand the exponential as follows:

$$\begin{aligned} F(q^2) &= \int \varrho(\vec{x}) \left(1 + i\vec{q}\cdot\vec{x} + (i\vec{q}\cdot\vec{x})^2 + ...\right) \mathrm{d}^3x \\ &= 1 - \frac{1}{6} \mid \vec{q} \mid^2 < r^2 > \quad . \end{aligned} \tag{183}$$

Here we have assumed that the charge distribution $\varrho(\vec{x})$ is spherical and depends only on $r \equiv \mid \vec{x} \mid$. The charge distribution is normalised to unity, and we also define the mean square radius $< r^2 >$ of the charge cloud:

$$\int \varrho(\vec{x}) \mathrm{d}^3 x = 1 \qquad\qquad < r^2 > = \int r^2 \varrho(r) \mathrm{d}^3 r$$

Thus for small q^2 which corresponds to small angle scattering the wavelength of the virtual photon transferred to the proton is large so that only the size of the proton can be resolved but not its internal structure.

As an example, an exponential charge distribution leads to the following dipole formula for the form factor:

$$\varrho(r) = \varrho_0 \exp(-r/r_0) \qquad \Longrightarrow \qquad F(q^2) = \left(\frac{1}{1 + \mid \vec{q} \mid^2 r_0^2} \right)^2 . \tag{184}$$

10.2 Elastic $e^- p \to e^- p$ Scattering

Here we describe a more general formalism for elastic $e^- p \to e^- p$ scattering. This approach was introduced before the structure of the proton was understood and is very general. In lowest order QED, this process can be described by the following Feynman diagram (Figure 46). Again the

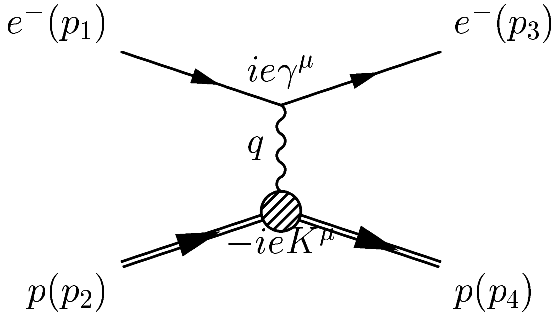

Figure 46: Elastic $e^- p \to e^- p$ scattering.

blob reminds us that we do not know how the virtual photon interacts with the proton. The matrix element can be written analogous to $\mathcal{M}(e^-\mu^- \to e^-\mu^-)$.

$$\mathcal{M}(e^- p \to e^- p) = \frac{+e^2}{(p_1 - p_3)^2} \left(\bar{u}_3 \gamma^\mu u_1 \right) \left(\bar{u}_4 K_\mu u_2 \right) \equiv \frac{1}{q^2} j_e{}^\mu j_{p_\mu} \tag{185}$$

The electron current and the propagator are left unchanged, but the muon current and muon-photon vertex are replaced by the corresponding proton-photon vertex current $j_p{}^\mu = e \left(\bar{u}_4 K^\mu u_2 \right)$.

We look first at the kinematics of $e^- p \to e^- p$ scattering. Working in the laboratory frame where the proton with mass M is at rest, we define the energy transfer ν, and the momentum transfer $\vec{q}$ to the proton

$$\nu \equiv E_1 - E_3 \qquad\qquad q \equiv (\nu, \vec{q}) . \tag{186}$$

Using four-momentum conservation at the proton-photon vertex we can derive the following relation between these q^2 and ν:

$$\begin{aligned} (q+p_2)^2 &= p_4^2 & p_2 \cdot q &= (M, \vec{0}) \cdot (\nu, \vec{q}) \\ q^2 + M^2 + 2p_2 \cdot q &= M^2 & &= M\nu \\ \Longrightarrow \qquad q^2 &= -2M\nu < 0 \end{aligned} \tag{187}$$

We realize that q^2 and ν are not independent variables, the energy E_3 of the scattered electron and the angle θ between the e^- beam direction and the scattered electron are related. Only the energy E_1 of the e^- beam and the scattering angle θ need to be measured to obtain the full kinematic information. Note that the mass squared of the virtual photon, q^2, is always negative for $e^-p \to e^-p$ scattering.

Since the proton is an extended structure we know that K^μ in Equation 185 is more complex than γ^μ. But the proton current j_p^μ which describes the vertex "blob" must be a four-vector. We then build the most general four-vector that can be constructed from p_2^μ, p_4^μ, q^μ and the Dirac matrices, γ^μ and $\sigma^{\mu\nu} = i/2(\gamma^\mu\gamma^\nu - \gamma^\nu\gamma^\mu)$. Not all of these are independent and the most general form reduces to

$$j_p^\mu = e\bar{u}(p_4)\left(\gamma^\mu F_1(q^2) + \frac{i\kappa}{2M}F_2(q^2)\sigma^{\mu\nu}q_\nu + q^\nu F_3(q^2)\right)u(p_2) \tag{188}$$

where we have introduced the three independent form factors F_1, F_2 and F_3 which are functions of q^2, the only available Lorentz scalar. Note that κ is the *anomalous magnetic moment* of the proton defined by $\mu_p = (1+\kappa)e/2M$. The conservation of the current $\delta_\mu j_p^\mu = 0$ implies that $F_3 = 0$. In the limit of $q^2 \to 0$, the form factors are normalised to unity

$$F_1(0) = 1 \qquad F_2(0) = 1 \qquad \kappa = +1.79 \qquad F_3 = 0\,.$$

When we probe the proton with long wavelength photons we observe a particle with charge e and magnetic moment $\mu_p = +2.79e/2M$. We can also define corresponding form factors for the neutron which, at $q^2 = 0$, will have the values

$$F_1(0) = 0 \qquad F_2(0) = 1 \qquad \kappa = -1.91 \qquad F_3 = 0\,.$$

We can now calculate the differential cross section for electron-proton scattering and obtain

$$\left.\frac{\mathrm{d}\sigma}{\mathrm{d}\Omega}\right|_{\mathrm{lab}} = \frac{\alpha^2}{4E_1^2\sin^4\frac{\theta}{2}}\frac{E_3}{E_1}\left\{\left(F_1^2 - \frac{\kappa^2q^2}{4M^2}\right)\cos^2\frac{\theta}{2} - \frac{q^2}{2M^2}\left(F_1+\kappa F_2\right)^2\sin^2\frac{\theta}{2}\right\} \tag{189}$$

This is known as the Rosenbluth formula. The two form factors $F_{1,2}(q^2)$ parameterise the structure of the proton and have to be determined by experiment. Note that for a point-like spin $\frac{1}{2}$ particle, $F_1(q^2) = 1$ and $\kappa = 0$, and Equation 189 reduces to

$$\left.\frac{\mathrm{d}\sigma}{\mathrm{d}\Omega}\right|_{\mathrm{lab}} = \frac{\alpha^2}{4E_1^2\sin^4\frac{\theta}{2}}\frac{E_3}{E_1}\left\{\cos^2\frac{\theta}{2} - \frac{q^2}{2M^2}\sin^2\frac{\theta}{2}\right\} \tag{190}$$

It is practical to use linear combinations of the form factors $F_{1,2}$

$$G_E = F_1 + \frac{\kappa q^2}{4M^2} F_2 \qquad\qquad G_M = F_1 + \kappa F_2$$

so that no interference terms $G_E G_M$ appear in the cross section. The Rosenbluth formula can be rewritten as

$$\left.\frac{\mathrm{d}\sigma}{\mathrm{d}\Omega}\right|_{\mathrm{lab}} = \frac{\alpha^2}{4E_1^2 \sin^4\frac{\theta}{2}} \frac{E_3}{E_1} \left(\frac{G_E^2 + \tau G_M^2}{1+\tau} \cos^2\frac{\theta}{2} + 2\tau G_M^2 \sin^2\frac{\theta}{2} \right) \tag{191}$$

where we have used the abbreviation $\tau = -q^2/4M^2$.

The quantities G_E and G_M are referred to as *electric* and *magnetic* form factor, respectively. In Figure 47, we show experimental data on G_E as a function of $-q^2$. The data are in good

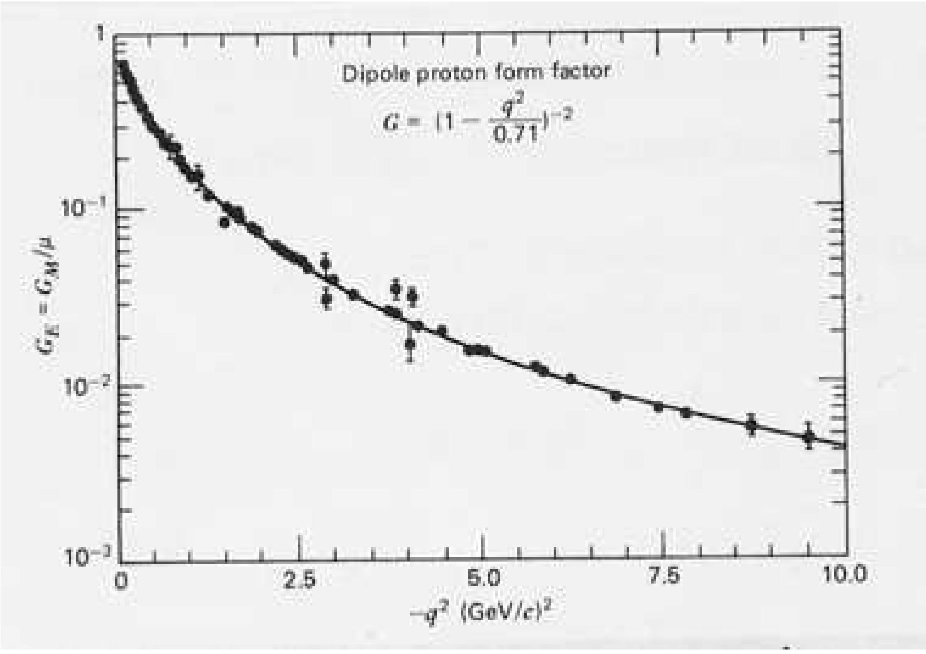

Figure 47: The proton form factor G_E as a function of $-q^2$.

agreement with the dipole formula, discussed above (see Equation 184). A fit yields a value of $M_V^2 = 1/r_0^2 = 0.71\,\mathrm{GeV}^2$ for the dipole mass. The behaviour at small q^2 can be used to extract information about the size of the proton. We conclude that the charge distribution within the proton has an exponential shape and that the proton has a mean charge radius of

$$< r^2 >= 6 \left(\frac{\mathrm{d}G_E(q^2)}{\mathrm{d}q^2} \right)_{q^2=0} = (0.81\,\mathrm{fm})^2 \,.$$

10.3 Deep Inelastic Scattering

To have a closer look at the structure of the proton, the momentum transfer $\mid \vec{q}^2 \mid$ must be increased. However, the proton often breaks up into hadrons at these high energies. The process becomes inelastic scattering, $e^- p \to e^- X$, as is shown in Figure 48. For medium $\mid \vec{q}^2 \mid$ one produces

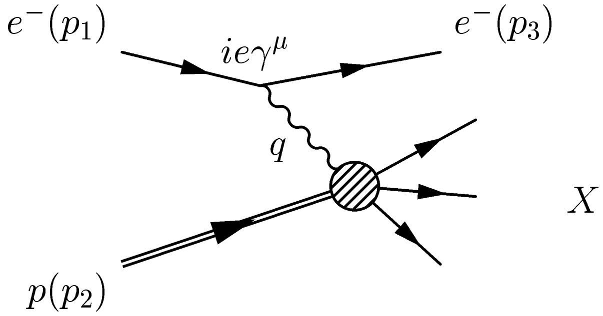

Figure 48: Deep Inelastic $e^- p \to e^- X$ scattering (DIS).

resonances such as $e - p \to e^- \Delta^+(1232) \to e^- p \pi^0$, which yield additional pions. At very large $\mid \vec{q}^2 \mid$ however, the proton turns into a very messy final state with many particles. We call this process **deep inelastic scattering** (DIS).

A new formalism is necessary to describe $e^- p \to e^- X$ scattering at very high energies. The four-momentum and energy transfer, q^2 and ν, are no longer independent in DIS, and consequently, E_3 and θ are not related anymore. One must measure E_1, E_3 and θ to determine the full DIS kinematics. It is useful to introduce the dimensionless variables x and y which replace ν and q^2

$$x = \frac{-q^2}{2M\nu} \qquad \text{Bjorken } x \qquad\qquad y = \frac{p_2 \cdot q}{p_2 \cdot p_1} \tag{192}$$

$$0 \leq x \leq 1 \qquad\qquad\qquad 0 \leq y \leq 1$$

where the allowed kinematics ranges for x and y are also given We define the mass of the hadronic final state system, X, as follows:

$$W^2 = q^2 + M^2 + 2M\nu$$

Note that generally the X particles are not detected and that the hadronic mass W is determined by measuring the electron energies E_1, E_3 and the scattering angle θ.

In deep inelastic scattering the proton breaks up into a X system of many particles. Thus the hadronic current in the matrix element must have a more complex structure. The matrix element squared can be factorised into

$$\langle \mid \mathcal{M} \mid^2 \rangle = \frac{e^4}{q^2} L_e^{\mu\nu} (W_{\mathrm{hadron}})_{\mu\nu}$$

where the leptonic tensor $L_e^{\mu\nu} = (\bar{u}_3 \gamma^\mu u_1)\,(\bar{u}_3 \gamma^\nu u_1)^*$ is known from electron-muon scattering and the hadronic tensor $W_{\mathrm{hadron}}^{\mu\nu}$ describes the $pX\gamma$ current. The calculation proceeds now in a similar way as for elastic $e^- p$ scattering. The hadronic tensor $W^{\mu\nu}_{\rm hadron}$ is constructed in the most general way possible

$$W^{\mu\nu}_{\rm hadron} = -W_1 g^{\mu\nu} + \frac{W_2}{M^2} p_2^\mu p_2^\nu + \frac{W_4}{M^2} q^\mu q^\nu + \frac{W_5}{M^2}\left(p_2^\mu q^\nu + q^\mu p_2^\nu\right)$$

Here we have introduced the **structure functions** W_1, W_2, W_4, and W_5 which are functions of the two independent Lorentz scalars q^2 and $p_2 \cdot q$. The latter is equivalent to the energy transfer $\nu = p_2 \cdot q/M$. Since W_4 and W_5 can be expressed as combinations of W_1 and W_2, we end up with two independent structure functions $W_1(\nu, q^2)$ and $W_2(\nu, q^2)$.

In the laboratory frame, we obtain the double differential cross section for deep inelastic $e^- p \to e^- X$ scattering

$$\left.\frac{{\rm d}\sigma}{{\rm d}E_3 {\rm d}\Omega}\right|_{\rm lab} = \frac{\alpha^2}{4E_1^2 \sin^4\frac{\theta}{2}}\left(W_2(\nu, q^2)\cos^2\frac{\theta}{2} + 2W_1(\nu, q^2)\sin^2\frac{\theta}{2}\right) \tag{193}$$

The structure functions $W_1(\nu, q^2)$ and $W_2(\nu, q^2)$, which depend on both q^2 and ν, describe the structure inside the proton. In modern language, these constituents are quarks and gluons, but the formalism is generally valid and was developed before quarks were established. In Figure 49, we show the double differential cross section as a function of the hadronic mass W, where W has

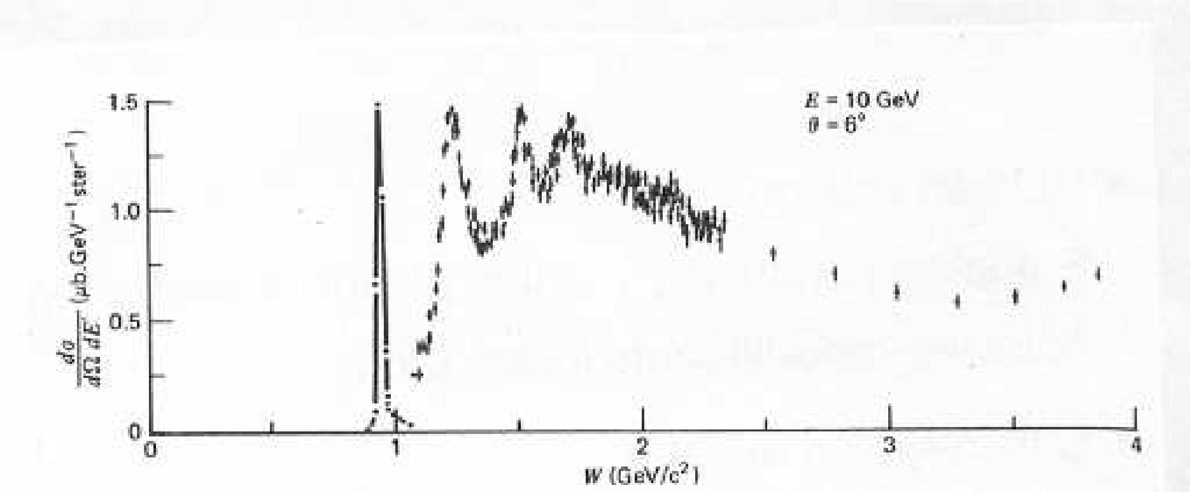

Figure 49: The $e^- p \to e^- X$ cross section as function of the missing mass W. Note that the elastic peak at $W = M$ has been reduced by a factor of 8.5.

been determined by measuring the electron energies E_1, E_3 and the scattering angle θ. Due to the energy transfer ν to the proton, the structure functions are not directly related to the Fourier transform of the charge distribution at $q^2 = 0$.

10.4 Scaling

Experimentally it was observed that to a good approximation the structure functions only depend on the ratio of q^2 and ν. Bjorken had predicted that at very high energy the structure functions become independent of q^2, hence the variable name "Bjorken" $x = -q^2/2M\nu$". He suggested that for deep inelastic scattering

$$MW_1(\nu, q^2) \to F_1(x) \qquad\qquad \nu W_2(\nu, q^2) \to F_2(x) \tag{194}$$

the structure functions $F_1(x)$ and $F_2(x)$[30] are functions of x alone, as is confirmed in experimental data (Figure 50). This behaviour is known as **Bjorken scaling**. If there are point-like spin $\frac{1}{2}$

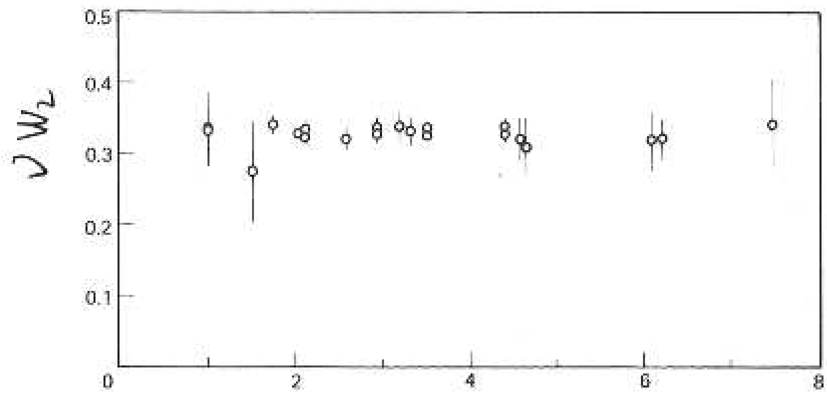

Figure 50: Scaling behaviour of the structure function $F_2 = \nu W_2$ as a function of $-q^2$ in deep inelastic scattering.

objects inside the proton, for very large negative q^2, the virtual photon is scattering off these constituents. We can treat this as elastic scattering of the electron on a "free" particle inside the proton. For point-like objects inside the proton, the structure functions become delta functions

$$2W_1 = \frac{-q^2}{2m^2}\delta(\nu - \frac{-q^2}{2m}) \qquad\qquad W_2 = \delta(\nu - \frac{-q^2}{2m}) \tag{195}$$

Later the Callan-Gross relation was found which relates the two structure functions $F_1(x)$ and $F_2(x)$ by

$$2xF_1(x) = F_2(x) \tag{196}$$

10.5 Parton Model

Feynman coined the name **partons** for the point-like constituents inside the nucleon. At the time, quarks and gluons were not yet established. We can obtain expressions for $F_1(x)$ and $F_2(x)$ by assuming that the underlying process is scattering a highly virtual photon off a parton, as is shown in Figure 51. The main assumption is that a high $| q^2 |$ interaction, partons can be treated

[30]Note that the Bjorken structure functions $F_1(x)$ and $F_2(x)$ are different from the elastic form factors F_1 and F_2.

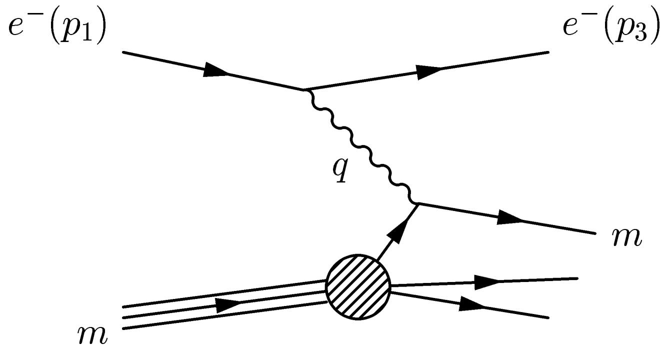

Figure 51: Parton Model.

as "free" particles with mass m inside a proton. This restores the dependence between q^2 and ν (see Equation 187)

$$\nu + \frac{q^2}{2m} = 0$$

and we can write down the cross section for elastic $e^-q \to e^-q$ scattering

$$\left.\frac{\mathrm{d}\sigma}{\mathrm{d}\Omega}\right|_{\mathrm{lab}} = \frac{e_q^2\alpha^2}{4E_1^2\sin^4\frac{\theta}{2}}\frac{E_3}{E_1}\left(\cos^2\frac{\theta}{2} - \frac{q^2}{2m^2}\sin^2\frac{\theta}{2}\right) \tag{197}$$

where e_q is the charge of the quark in units of e.

We obtain a relation between the Bjorken x and the parton mass m:

$$\nu + \frac{q^2}{2m} = 0 \qquad x = \frac{-q^2}{2M\nu} \qquad \Longrightarrow \qquad x = m/M\ . \tag{198}$$

In the laboratory frame where the proton is at rest, x is a fraction of the proton mass M. In the *infinite momentum frame* where the proton has a large momentum, each parton carries a fraction x of the protons momentum $\vec{p}$ and energy E

$$m^2 = x^2E^2 - x^2\vec{p}^2 = x^2M^2$$

Now we introduce the parton **momentum distribution function**, $f_i(x)$, defined as the probability that a parton i carries a momentum fraction x. All the parton momentum fractions must add up to unity

$$\Sigma_i\int x f_i(x)\mathrm{d}x = 1\ .$$

By integrating the over the delta functions (Equation 195) we obtain for the structure functions (Equation 194)

$$2W_1(x) = \Sigma_i\int_0^1\frac{-q_i^2}{2m}\delta(\nu - \frac{-q_i^2}{2m})f_i(x)\mathrm{d}x = \frac{1}{2M}\Sigma_i(-q_i^2)f_i(x) \equiv \frac{F_1(x)}{M}$$
$$W_2(x) = \Sigma_i\int_0^1\delta(\nu - \frac{-q_i^2}{2m})f_i(x)\mathrm{d}x = \frac{1}{\nu}\Sigma_i(-q_i^2)xf_i(x) \equiv \frac{F_2(x)}{\nu}$$

It follows that the two structure functions F_1 and F_2 are related by

$$2xF_1(x) = F_2(x) = \sum_i e_i^2 x f_i(x)$$

which is the aforementioned Callan-Gross relation. The function $F_2(x)$ is equal to the momentum distribution function weighted by the momentum fraction and the charge squared of the partons, summed over all partons in the proton.

Let $u(x)$ be the probability that the u quark has a momentum fraction x within the proton, and that $d(x)$ is the probability that the d quark has a momentum fraction x in the p. The normalisations are chosen as follows:

$$\int_0^1 u(x)\mathrm{d}x = 2 \qquad\qquad \int_0^1 d(x)\mathrm{d}x = 1 \ .$$

This allows us to calculate the structure function $F_2^{ep}(x)$. For the 3 valence quarks uud we obtain

$$F_2^{ep}(x) = \sum_i e_i^2 x f_i(x) = \frac{4}{9}xu(x) + \frac{1}{9}xd(x) \ .$$

It turns out that in addition to the valence quarks there is a *sea* of $q\bar{q}$ pairs within the proton. This contribution has to be added. We introduce the additional distribution functions $\bar{u}(x)$ and $\bar{d}(x)$ and obtain

$$F_2^{ep}(x) = x\left(\frac{4}{9}u(x) + \frac{1}{9}d(x) + \frac{4}{9}\bar{u}(x) + \frac{1}{9}\bar{d}(x)\right)$$

where we have neglected the contributions of heavier quark pairs, $s\bar{s}$ and $c\bar{c}$ to the sea.

The structure of the neutron can be obtained by comparing DIS measurement for deuterium and proton targets. Using isospin symmetry we predict that when comparing neutrons with protons, $u(x)$ must be exchanged with $d(x)$ and vice versa. We obtain the structure function for the neutron valence quarks ddu:

$$F_2^{en}(x) = \sum_i e_i^2 x f_i(x) = \frac{4}{9}xd(x) + \frac{1}{9}xu(x)$$

In Figure 52, we show the quark structure functions as a function of x, as measured from DIS. The right-hand side plot show the total valence and the sea quark distributions to the proton.

We integrate the area under the structure function $F_2(x)$ to measure the total momentum fraction carried by the quarks within the proton. We write the integral as follows

$$\int_0^1 F_2^{ep}(x)dx = \frac{4}{9}f_u + \frac{1}{9}f_d \qquad\qquad \int_0^1 F_2^{en}(x)dx = \frac{4}{9}f_d + \frac{1}{9}f_u$$

where f_u is the fraction of the proton momentum carried by u and $\bar{u}$ quarks, and f_d is the fraction carried by d and $\bar{d}$ quarks, respectively.

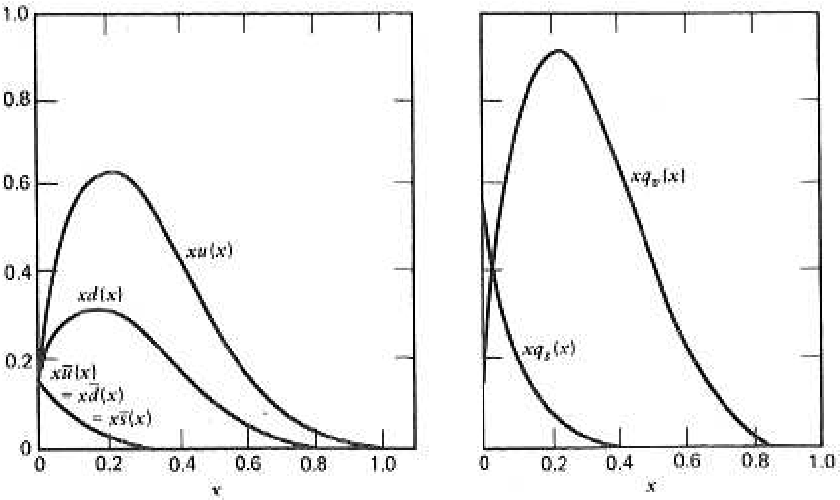

Figure 52: Quark structure functions. The right-hand side plot shows the total valence and sea quark contributions to the proton structure.

The measurements of the integrated structure function produces the following surprising result:

$$\begin{aligned} \int_0^1 F_2^{ep}(x)dx &= 0.18 \\ \int_0^1 F_2^{en}(x)dx &= 0.12 \end{aligned} \quad \Longrightarrow \quad \begin{aligned} f_u &= 0.36 \\ f_d &= 0.18 \end{aligned} \tag{199}$$

The quarks carry only 54 % of the proton momentum. The remaining momentum is carried by the gluons. Hence, partons are identified as and comprise of both, quarks and gluons. In Figure 53, the structure function $F_2^{ep}(x)$ is sketched for different assumed compositions of a proton.

Precision measurements show small deviations from exact Bjorken scaling, i.e. there is a small dependence on q^2. These **scaling violations** are expected at large q^2. Quarks share their momenta with gluons. We plot a summary for measurements of $F_2(x)$ in fixed target experiments. At the HERA $e^{\pm}p$ collider, 30 GeV electrons or positrons collide with 820 GeV protons. This machine has allowed to explore regions of larger $|q^2|$ and lower x as is shown in Figure 55.

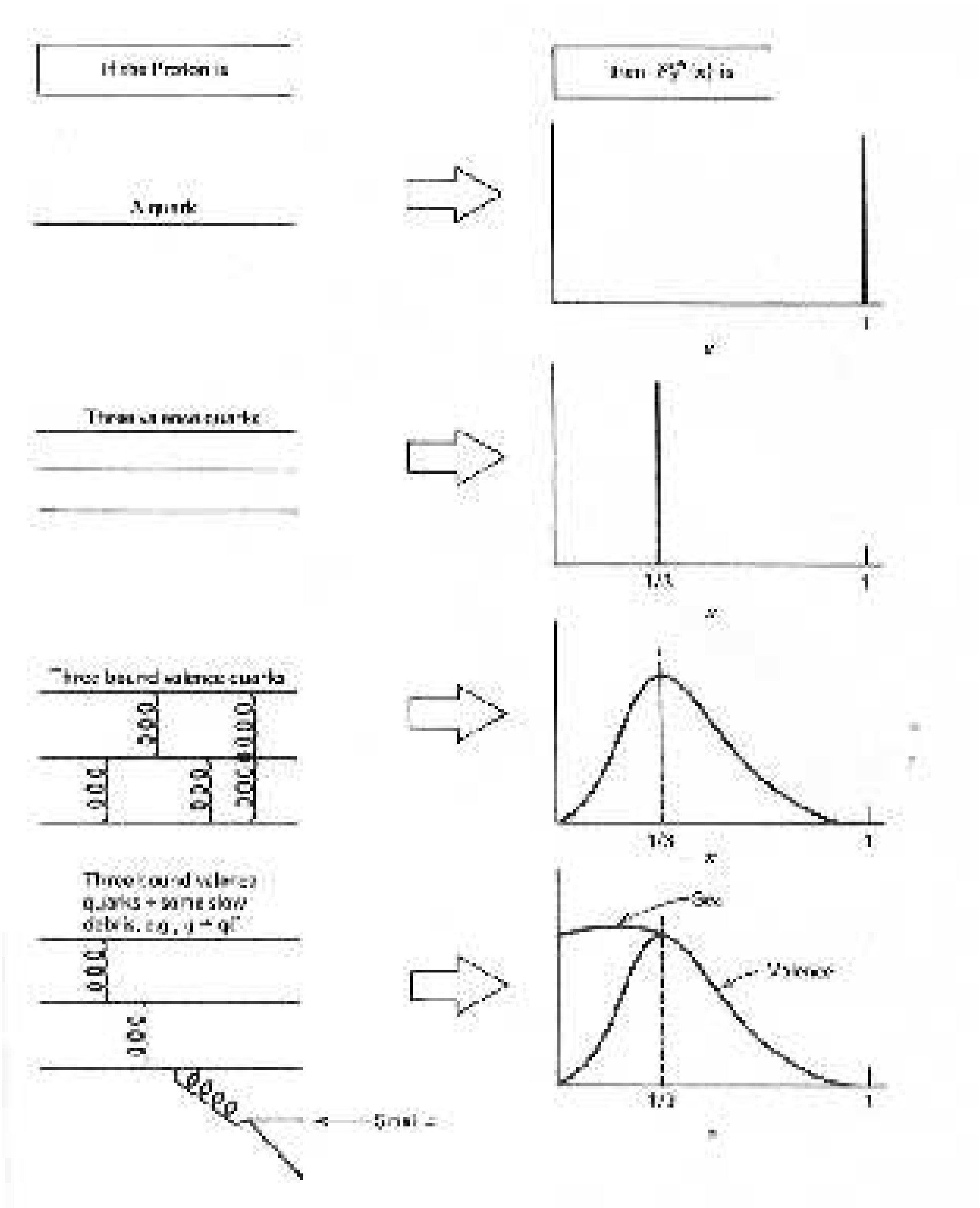

Figure 53: Structure functions $F_2(x)$ for different compositions assumed for the proton.

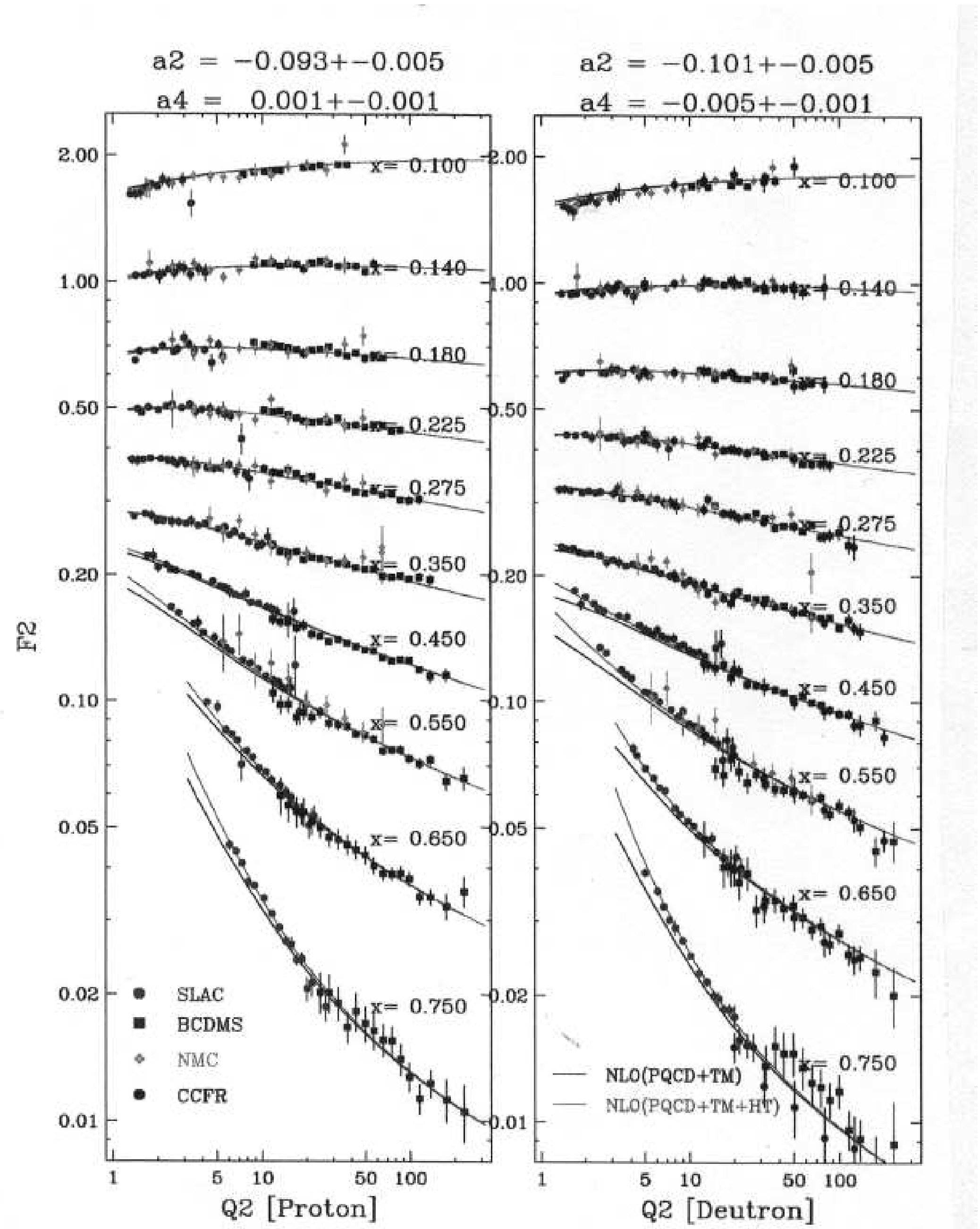

Figure 54: Summary of structure functions $F_2(x)$ for fixed target data which show scaling violations.

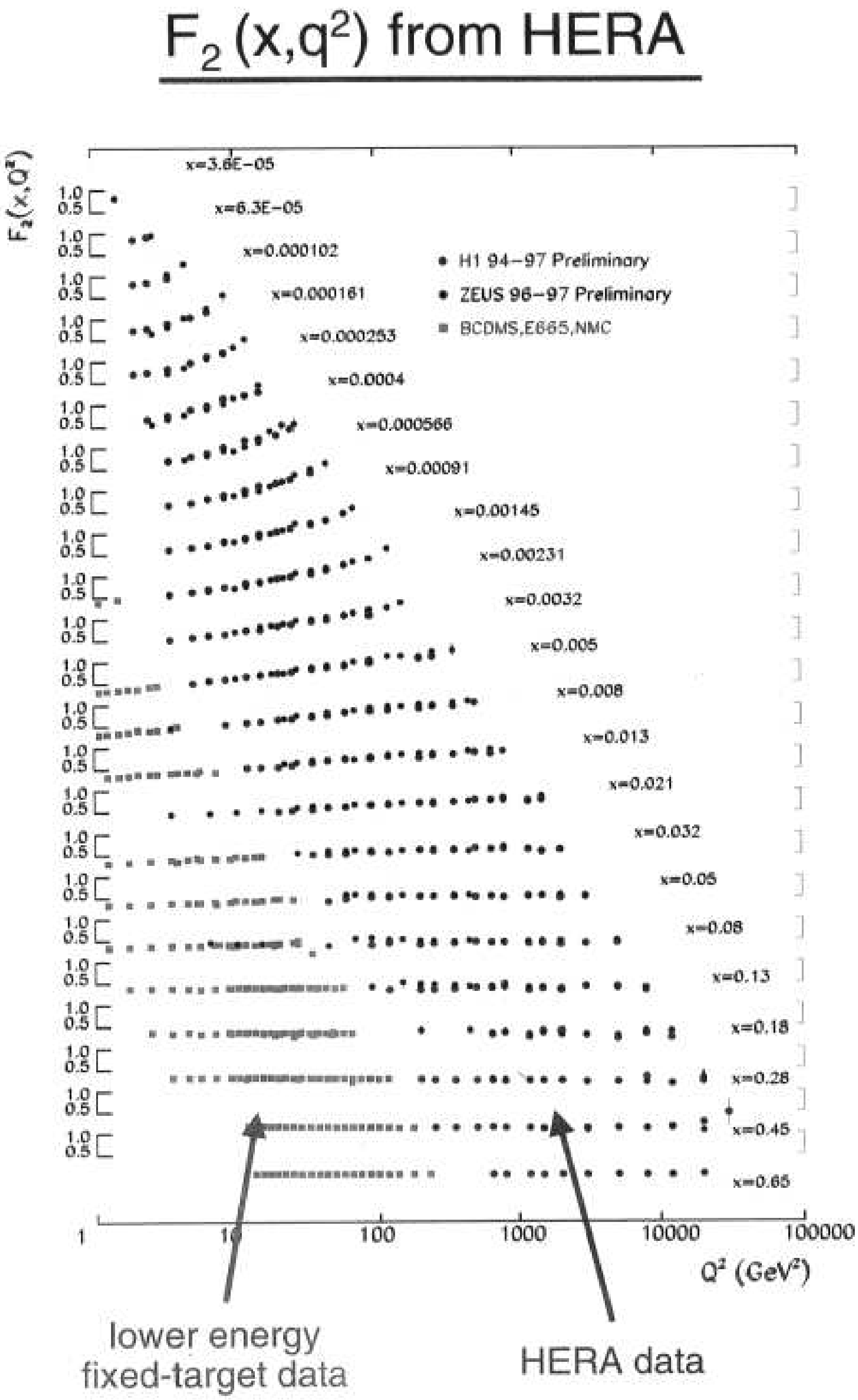

Figure 55: Structure functions $F_2(x)$ measured at HERA.